JOURNAL OF VIROLOGY, June 2006, p. 5423–5434 Vol. 80, No. 11
0022-538X/06/$08.00+0 doi:10.1128/JVI.02585-05

Deletion of Open Reading Frame UL26 from the Human Cytomegalovirus Genome Results in Reduced Viral Growth, Which Involves Impaired Stability of Viral Particles

Kerstin Lorz,[1] Heike Hofmann,[1]† Anja Berndt,[1] Nina Tavalai,[1] Regina Mueller,[1] Ursula Schlötzer-Schrehardt,[2] and Thomas Stamminger[1]*

Institute of Clinical and Molecular Virology, University of Erlangen-Nuernberg, Schlossgarten 4, 91054 Erlangen, Germany,[1] and Department of Ophthalmology, University of Erlangen-Nuernberg, Schwabachanlage 6, 91054 Erlangen, Germany[2]

Received 13 December 2005/Accepted 10 March 2006

We previously showed that open reading frame (ORF) UL26 of human cytomegalovirus, a member of the US22 multigene family of betaherpesviruses, encodes a novel tegument protein, which is imported into cells in the course of viral infection. Moreover, we demonstrated that pUL26 contains a strong transcriptional activation domain and is capable of stimulating the major immediate-early (IE) enhancer-promoter. Since this suggested an important function of pUL26 during the initiation of the viral replicative cycle, we sought to ascertain the relevance of pUL26 by construction of a viral deletion mutant lacking the UL26 ORF using the bacterial artificial chromosome mutagenesis procedure. The resulting deletion virus was verified by PCR, enzyme restriction, and Southern blot analyses. After infection of human foreskin fibroblasts, the UL26 deletion mutant showed a small-plaque phenotype and replicated to significantly lower titers than wild-type or revertant virus. In particular, we noticed a striking decrease of infectious titers 7 days postinfection in a multistep growth experiment, whereas the release of viral DNA from infected cells was not impaired. A further investigation of this aspect revealed a significantly diminished stability of viral particles derived from the UL26 deletion mutant. Consistent with this, we observed that the tegument composition of the deletion mutant deviates from that of the wild-type virus. We therefore hypothesize that pUL26 plays a role not only in the onset of IE gene transcription but also in the assembly of the viral tegument layer in a stable and correct manner.

Human cytomegalovirus (HCMV), a member of the betaherpesvirus family, is characterized by its narrow host range and prolonged replicative cycle in cell culture as well as in the infected human host. In immunocompetent individuals, HCMV causes mainly asymptomatic infections, whereas in immunocompromised or immunosuppressed individuals, acute or reactivated infection often leads to severe courses comprising pneumonitis, retinitis, or hepatitis. Serious complications, including neurological symptoms, can also arise from congenital infection of newborns (20, 22, 43). As for other herpesviruses, HCMV is able to establish both lytic and latent infections and remains persistent in its host lifelong after primary infection (reviewed in reference 33). Gene expression during lytic HCMV replication follows a strictly coordinated pattern, proceeding in three phases characteristic for the herpesvirus family, termed immediate-early (IE), early, and late (18, 25, 49). Initial viral transcription mainly involves the major immediate-early gene region (MIE region), which encodes a number of proteins with *trans*-regulatory functions. Best known examples are the immediate-early proteins IE1p72 and IE2p86, which are both involved in the activation of promoters of the early phase (21, 34, 46). The MIE region is controlled by the major immediate-early enhancer-promoter (MIEP), which contains several recognition sites for eukaryotic transcription factors such as NF-κB and Sp1 (for a review, see reference 26).

Activation of IE transcription, however, is also mediated by structural protein components of the incoming virion itself (12, 24, 38, 39). Those proteins are located in the tegument layer, a structure unique for herpesviruses, which encloses the nucleocapsid and separates it from the lipid envelope. Tegument proteins are thought to play an important role in the onset of viral replication. For instance, pp71(UL82), a component of the tegument, is capable of activating IE gene expression in infected cells via stimulation of the HCMV MIEP (12). Two other tegument proteins, ppUL69 and ppUL35, activate the major IE enhancer-promoter synergistically in interplay with pp71(UL82) (39, 50).

We and others have previously shown that the UL26 open reading frame (ORF) encodes an additional tegument protein, termed pUL26, which is expressed in two isoforms of 21 and 27 kDa (7, 44, 47). pUL26 is present during the IE phase of the viral replication cycle due to protein import by the viral inoculum and is able to transactivate the HCMV MIEP about 10-fold but does not stimulate early and late viral promoters (44).

Recently, pUL26 was assigned to the US22 multigene family (17). Members of the US22 family contain one to four characteristic sequence motifs and can be found in all known members of the *Betaherpesvirinae* but not in *Alphaherpesvirinae* and *Gammaherpesvirinae* (31). US22 proteins exert functions in the inhibition of apoptosis (42) as well as the regulation of gene expression (16, 45). As pUL26 shows features of other known regulators of viral gene expression located in the viral tegu-

* Corresponding author. Mailing address: Institut für Klinische und Molekulare Virologie, Schlossgarten 4, 91054 Erlangen, Germany. Phone: 49 9131 852 6783. Fax: 49 9131 852 2101. E-mail: thomas.stamminger@viro.med.uni-erlangen.de.

† Present address: Institut für Infektionsmedizin, Universitätsklinikum Schleswig-Holstein Campus Kiel, Brunswiker Str. 4, 24105 Kiel, Germany.

ment (transactivation capacity and protein import during infection), we wanted to further determine the role of pUL26 in the regulation of HCMV replication by means of construction of a recombinant virus with a deletion of the UL26 ORF.

In this report, we describe the construction and characterization of ΔUL26, a virus that lacks the entire UL26 sequence. This mutant virus exhibited a growth defect that could be repaired by the reinsertion of the UL26 ORF. We present evidence that the ΔUL26 virus is less infectious than wild-type virus due to a reduced stability of viral particles lacking pUL26. Moreover, we observed that the tegument composition of the deletion mutant deviates from that observed with the wild-type virus. Thus, our results suggest that pUL26 exerts an important function for assembly of the viral tegument layer in a stable and correct manner.

MATERIALS AND METHODS

Cells and viruses. Human foreskin fibroblast (HFF) cells were maintained in Eagle's minimal essential medium (GIBCO/BRL, Eggenstein, Germany) supplemented with 5% fetal calf serum and were used between passages 6 and 15. The cytomegalovirus strain employed in this study as a control for growth kinetic analyses was obtained by reconstitution of infectious viruses using the bacterial artificial chromosome (BAC) pHB15, which contains the genomic sequence of HCMV laboratory strain AD169 (kindly provided by G. Hahn, Munich, Germany) (23). For preparation of virus stocks, HFF cells were infected at a multiplicity of infection (MOI) of <0.01 and incubated in a humidified 5% CO_2 atmosphere at 37°C for about 7 to 14 days until the cultures displayed a complete cytopathic effect (CPE). Supernatants were collected, cleared by centrifugation for 10 min at 2,000 rpm, and stored in aliquots at −80°C. In order to obtain high-titered stocks of the ΔUL26 virus, viral supernatants were concentrated using Vivaspin ultrafiltration spin columns (molecular weight cutoff, 300,000) prior to storage at −80°C (Vivascience, Hannover, Germany). Virus stocks were titrated by IE1p72 fluorescence as described previously (4). Briefly, HFFs were infected with various dilutions of virus stocks. After 24 h of incubation, cells were fixed and stained with monoclonal antibody (MAb) p63-27 directed against IE1p72 (4). Subsequently, the number of positive cells was determined, and viral titers were calculated. Alternatively, viral stocks were titrated based on genomic equivalents imported into cells by infection. For this, cells were infected with various amounts of viral inocula followed by the preparation of genomic DNA 12 h postinfection using the DNeasy tissue kit (QIAGEN, Hilden, Germany). Real-time PCR (see below) was then performed for quantification of HCMV DNA. In subsequent experiments, viral inocula were normalized for infection to yield equivalent amounts of viral genomes per cell.

For analysis of growth kinetics of recombinant viruses, HFF cells were infected 24 h after seeding (3×10^5 cells/six-well dish) in triplicate at 0.1 or 0.01 infectious units/cell for a multistep growth curve. Samples were taken at 1, 3, 5, 7, 9, and 12 days after infection for titration as described above. For analysis of plaque formation, HFF cells were cultivated in six-well dishes and infected at 0.00025, 0.0005, or 0.001 infectious units/cell with HB15, ΔUL26, and the UL26 revertant virus. After 1 h of incubation, the viral inoculum was removed, and cells were covered with agar overlay medium and incubated at 37°C until the appearance of plaques. IE1p72-expressing cells were generated via retroviral transduction and blasticidin selection using the ViraPower lentiviral expression system with the coding sequence of IE1 cloned into the pLenti6/V5-D-Topo vector (Invitrogen, Karlsruhe, Germany). IE1p72 expression was confirmed by indirect immunofluorescence analysis using the monoclonal antibody p63-27. Plaque assays using IE1p72-expressing cells were performed by infection with 0.0005 infectious units/cell as described above.

To investigate the stability of virions, confluent HFF cells in 12-well dishes were infected with freshly thawed virus stocks (HB15, ΔUL26, and UL26 revertant) at 0.001 infectious units/cell in duplicates; the remaining material that was not used for infection was kept at 20°C and employed for infection of HFF cells during the subsequent 5 days. For quantification of the remaining infectivity, IE1p72-positive cells were counted for each well 48 h postinfection.

Purification of HCMV virus particles from the supernatant of infected HFF cells was performed when the cultures displayed a distinctive cytopathic effect. Supernatants were collected and cleared by centrifugation for 10 min at 2,000 rpm. After sedimentation of virus particles by ultracentrifugation (23,000 rpm, 10°C, 70 min; Beckman SW27 rotor) and resuspension in 0.04 M Na-phosphate buffer, pH 7.4, the pellets were loaded onto a glycerol-tartrate gradient (3) and again subjected to ultracentrifugation (23,000 rpm, 10°C, 70 min; Beckman SW27 rotor). The virion fraction obtained from the gradient was diluted in 0.04 M Na-phosphate buffer (pH 7.4), pelleted by centrifugation, and resuspended using the same buffer.

BAC isolation and plasmids for BAC mutagenesis. Small amounts of BAC DNA were isolated by a standard alkaline lysis procedure (36) from 5-ml cultures grown overnight. Large-scale BAC preparations were obtained from 500-ml cultures grown overnight using the Nucleobond AX 100 kit (Machery Nagel, Düren, Germany) according to the manufacturer's instructions.

For generation of the recombination vector pHM2086 for the deletion of the UL26 ORF, its 5′- and 3′-flanking regions were amplified by PCR (primers 5′-GCCTTATTAAGCCTGCTGCACGGCGCAC-3′ and 5′-GGGGTACCTTA ACGCGCCGCCGCGGC-3′ and 5′-GGGATATCCGGCAACGTGCCATCA GC-3′ and 5′-GGGATATCCCGGAATTCGGCCTTCGCGCTCACC-3′, respectively). The fragments were digested with either PacI and Asp718 (5′-flanking sequence of UL26) or EcoRV (3′-flanking sequence of UL26) and ligated into the respective sites of the pCP-O15 vector (15). An additional EcoRI restriction site was inserted into the 3′-flanking sequence to enable linearization of the recombination cassette, which additionally contained a kanamycin resistance gene flanked by *frt* sites.

For generation of the UL26 revertant BAC, the shuttle plasmid pHM1781 containing the UL26 ORF in the context of its genomic 5′- and 3′-flanking sequences was created by PCR amplification using the primers 5′-GGGGTAC CGCGGCATTGAAGGACC-3′ and 5′-CGGGATCCGCGAAGAGCACACG-3′. The fragment was digested with Asp718 and BamHI and ligated into the corresponding sites of the pST76K-SR vector, containing a kanamycin resistance gene, the recombinase gene *recA*, the *sacB* selection marker, and a temperature-sensitive origin of replication (35).

BAC mutagenesis. For construction of the ΔUL26 BAC, homologous recombination via a linear recombination cassette was performed. The linear recombination fragment necessary for mutagenesis (reviewed in reference 2) was excised from plasmid pHM2086 by EcoRI treatment and used for electroporation of competent *Escherichia coli* strain DH10B harboring the parental BAC pHB15 (23). The *E. coli* cells additionally contained the plasmid pBAD-αβγ, which inducibly expressed the recombination enzymes redα and redβ of phage λ (30). Bacterial clones harboring recombinant HCMV BACs were selected on agar plates containing 30 μg/ml kanamycin and 30 μg/ml chloramphenicol. After a first characterization of the recombinant HCMV BACs via restriction enzyme digestion and Southern blotting, the kanamycin resistance marker was removed by site-specific recombination in *E. coli* cells expressing Flp recombinase (15). The integrity of the resulting UL26 deletion mutants, termed pHM2091 (ΔUL26-2) and pHM2092 (ΔUL26-5), was further confirmed by restriction enzyme digestion, Southern blot, and PCR analyses. The UL26 revertant BAC with a reinserted UL26 ORF was generated by a two-step replacement mutagenesis procedure as described previously (27, 32). Briefly, shuttle plasmid pHM1781 was electroporated into *E. coli* DH10B containing a ΔUL26 BAC. Cointegrates between the BAC and the shuttle plasmid were selected by cultivation on agar plates containing 30 μg/ml chloramphenicol and 30 μg/ml kanamycin at 43°C. To allow resolution of the cointegrates, bacteria were selected on plates containing chloramphenicol and incubated at 37°C. Clones that had resolved their cointegrates were isolated by incubation on plates containing chloramphenicol plus 5% sucrose and subsequently tested for kanamycin sensitivity. This resulted in BACs pHM2104 (Rev-2) and pHM2105 (Rev-5), which were further analyzed for structural integrity as described above. Furthermore, the nucleotide sequence of the UL25-UL27 gene region of both mutated and revertant BACs was determined by automated sequence analysis (ABI, Weiterstadt, Germany) using a set of 14 sequencing primers that covered the entire UL25-UL27 gene region.

Reconstitution of recombinant cytomegaloviruses. One day before transfection, HFF cells were seeded into six-well dishes at a density of 3.5×10^5 cells/well. Transfection using SuperFECT reagent (QIAGEN, Hilden, Germany) was performed with 1 μg of the purified BAC DNA and expression plasmids for pp71(UL82) and for the Cre recombinase. The HCMV tegument protein pp71(UL82) was coexpressed since it is known to enhance the infectivity of viral DNA (6); coexpression of Cre recombinase is necessary in order to remove the BAC cassette and the chloramphenicol resistance gene, which are located between two *loxP* sites within the HCMV BAC pHB15 (23). One week after transfection, the cells were transferred into 25-cm^2 flasks and incubated until plaques appeared. After development of a nearly complete CPE, the supernatant was used for infection of fresh HFF cultures and preparation of virus stocks. The recombinant viruses employed in this study were termed ΔUL26 and Rev (UL26 revertant) and were derived from the BACs pHM2091 and pHM2104, respectively.

DNA, RNA, and protein analyses. For restriction enzyme analyses, BAC DNA was digested with enzymes for at least 4 h, loaded onto a 0.7% agarose gel, and separated via electrophoresis at 30 V overnight. For Southern blot analyses, the DNA was transferred onto nylon membranes (Biodyne B transfer membrane; PALL, Portsmouth, United Kingdom) and probed with biotinylated DNA against the UL25-UL27 region of HCMV according to the instructions of the manufacturer (NEBlot Phototope kit; Biolabs, Frankfurt, Germany). For characterization of BACs by PCR, reactions were performed directly from bacterial colonies according to standard amplification conditions using *Taq* polymerase in the presence of dimethyl sulfoxide and formamide. Primers were located either within the UL26 ORF (5′-ATGCGGATCCATGACGAGTAGGCGCGC-3′ and 5′-ATGCGATATCGTCGGCGTCGCGTGCG-3′), within the UL25 ORF (5′-TCGACGCCTACTAGGAACG-3′ and 5′-TGGCGACGATAACAGCAG C-3′), or within the UL27 ORF (5′-AGAAGACCATGACGACGG-3′ and 5′-TGCGTCCGGTACTTGACG-3′). RNA was isolated from virus-infected cells by using the High Pure RNA isolation kit (Roche Diagnostics, Mannheim, Germany). Reverse transcription was performed with the Reverse Transcription system according to instructions provided by the manufacturer (Promega GmbH, Mannheim, Germany), followed by PCR amplification of UL27 sequences using the UL27-specific primers that were also used for PCR characterization of BACs. As a control, RNA was used for PCR amplification without prior reverse transcription.

For real-time PCR, an aliquot of the supernatants from infected cells was incubated with proteinase K (Sigma, Deisenhofen, Germany) at 56°C for 1 h in order to release the viral DNA. Alternatively, DNA was extracted from virus-infected cells using the DNeasy tissue kit (QIAGEN, Hilden, Germany). After a denaturing step at 95°C for 5 min, the DNA samples were stored at 4°C. Real-time PCR was performed in a 25-μl reaction mixture containing 5 μl of either the sample or the standard DNA solution. Additional components of the reaction mixture were 12.5 μl 2× TaqMan PCR Mastermix (Applied Biosystems,), 7.5 pmol of each primer (5′-AAGCGGCCTCTGATAACCAAG-3′/ and 5′-GAGC AGACTCTCAGAGGATCG-3′), and 5 pmol probe directed against the HCMV MIE region exon 4 (5′-CATGCAGATCTCCTCAATGCGCGC-3′), which was labeled with 6-carboxyfluorescein reporter dye and 6-carboxytetramethylrhodamine quencher dye. The DNA standard for quantification was prepared by serial dilutions of plasmid pHM123 (5). The thermal cycling conditions consisted of two initial steps of 2 min at 50°C and 10 min at 95°C followed by 40 amplification cycles (15 s at 95°C, 1 min 60°C). Real-time PCR was performed with an ABI Prism 7700 sequence detector (Applied Biosystems). For each sample, DNA extracts were analyzed in triplicate.

For Western blotting, extracts from infected cells or virions were prepared in sodium dodecyl sulfate loading buffer, separated by sodium dodecyl sulfate-containing 8 to 15% polyacrylamide gels, and transferred onto nitrocellulose membranes (PROTRAN BR 83; Schleicher & Schuell, Dassel, Germany). Western blotting and chemiluminescence detection were performed according to the manufacturer's protocol (ECL Western detection kit; Amersham Pharmacia Biotech Europe, Freiburg, Germany). Antibodies against pUL26, pUL25, ppUL69, pp65(UL83) (MAb 65-33), UL84, pp28(UL99) (MAb 41-18), pp71(UL82), MCP(UL86) (MAb 28-4), IE2 (anti-pHM178), and IE1p72 (MAb p63-27) have been described previously (4, 8, 37, 44, 48, 51). The peroxidase-coupled secondary antibodies were purchased from Dianova (Hamburg, Germany).

Electron microscopy. For transmission electron microscopy, samples were fixed in buffered 2.5% glutaraldehyde solution for 24 h, postfixed in buffered 1% osmium tetroxide, dehydrated, and embedded in epoxy resin according to standard protocols. Ultrathin sections were stained with uranyl acetate and lead citrate. Viral particles, purified by ultracentrifugation on a glycerol-tartrate gradient as described above, were negatively stained using 3% uranyl acetate. Samples were examined with a LEO 906E electron microscope (Carl Zeiss NTS GmbH, Oberkochen, Germany).

RESULTS

Construction and verification of a mutant virus lacking the UL26 ORF. To elucidate the role of pUL26 in HCMV replication, we generated a deletion mutant lacking the entire UL26 open reading frame as predicted previously by Chee et al. (14). For construction of recombinant viruses, we employed BAC technology (reviewed in reference 2). The 5′- and 3′-flanking sequences of the UL26 gene were cloned into the recombination vector pCP-O15 (15), which contains a kanamycin gene as a resistance marker. The linearized recombination cassette was electroporated into bacteria harboring the HCMV AD169 genome as BAC (termed pHB15) as well as the pBAD plasmid encoding the recombination functions of phage λ (30) (for a detailed description, see Materials and Methods). After successful homologous recombination, the kanamycin cassette was excised at its flanking *frt* sites by Flp recombinase in bacteria, resulting in a BAC termed ΔUL26 (15). In order to generate a revertant virus, we reinserted the UL26 ORF into the ΔUL26 BAC by a two-step replacement procedure via the formation of cointegrates. For this, the UL26 ORF and its flanking sequences were cloned into the shuttle vector pST76K-SR (35), which confers sucrose sensitivity and contains a temperature-sensitive origin of replication. Subsequently, the recombination vector was electroporated into *E. coli* cells containing the ΔUL26 BAC, followed by several selection steps (see Materials and Methods). The integrity of the resulting ΔUL26 BACs or revertant BACs was first investigated by restriction enzyme cleavage with HindIII (Fig. 1A) and EcoRI (Fig. 1B). Both HindIII and EcoRI digestions of two independent ΔUL26 BACs (ΔUL26-2 and ΔUL26-5) and two UL26 revertant clones (Rev-2 and Rev-5) yielded complex patterns identical to those of pHB15 wild-type DNA, with the following predicted exceptions (Fig. 1A and B, marked with a white dot for ΔUL26 clones): HindIII digestion of ΔUL26 BACs produced a unique fragment of 8.1 kb due to the removal of the UL26 ORF (Fig. 1A, lanes 2 and 3), and EcoRI digestion of ΔUL26 BACs resulted in the disappearance of a 9.4-kb fragment and the appearance of an 8.9-kb fragment (Fig. 1B, lanes 2 and 3). Deletion or insertion of DNA fragments at the correct site of the HCMV genome was subsequently verified by Southern blot analyses using HindIII-digested (Fig. 1A, lower panel) or EcoRI-digested (Fig. 1B, lower panel) BAC DNA together with a biotinylated probe spanning the UL25-UL27 gene region. Consistent with the deletion of the UL26 ORF, this probe detected a faster-migrating fragment in ΔUL26 BACs (Fig. 1A and B, lanes 2 and 3, lower panels). In UL26 revertant clones, a fragment of the same size as those of pHB15 was observed (Fig. 1A and B, lanes 1, 4, and 5, lower panels). The scheme in Fig. 1D indicates the HindIII and EcoRI restriction sites in relation to the UL25-UL27 gene region. For additional characterization, PCRs were performed directly from bacterial colonies (Fig. 1C). The location of primer pairs in relation to the recombination cassette as well as expected fragment sizes are depicted at the bottom of Fig. 1C. Three primer pairs were employed, one of which was located within the UL26 ORF, one of which was located within the UL25 ORF, and one of which was located within the UL27 ORF. Concerning the UL25 and UL27 ORFs, one of the oligonucleotides was located within the recombination cassette, and the second was located outside of the recombination cassette. As expected, no PCR fragments were obtained for ΔUL26 BACs using the UL26 primers. All fragments amplified from the recombinant BACs displayed the predicted sizes. Finally, the correct nucleotide sequence of the UL25-UL27 gene region of both the deleted and the revertant BAC clones was confirmed by nucleotide sequence analysis. Taken together, the results of Southern blot, PCR, and nucleotide sequence analyses showed that recombination events took place at the correct sites of the HCMV genome. Thus, we

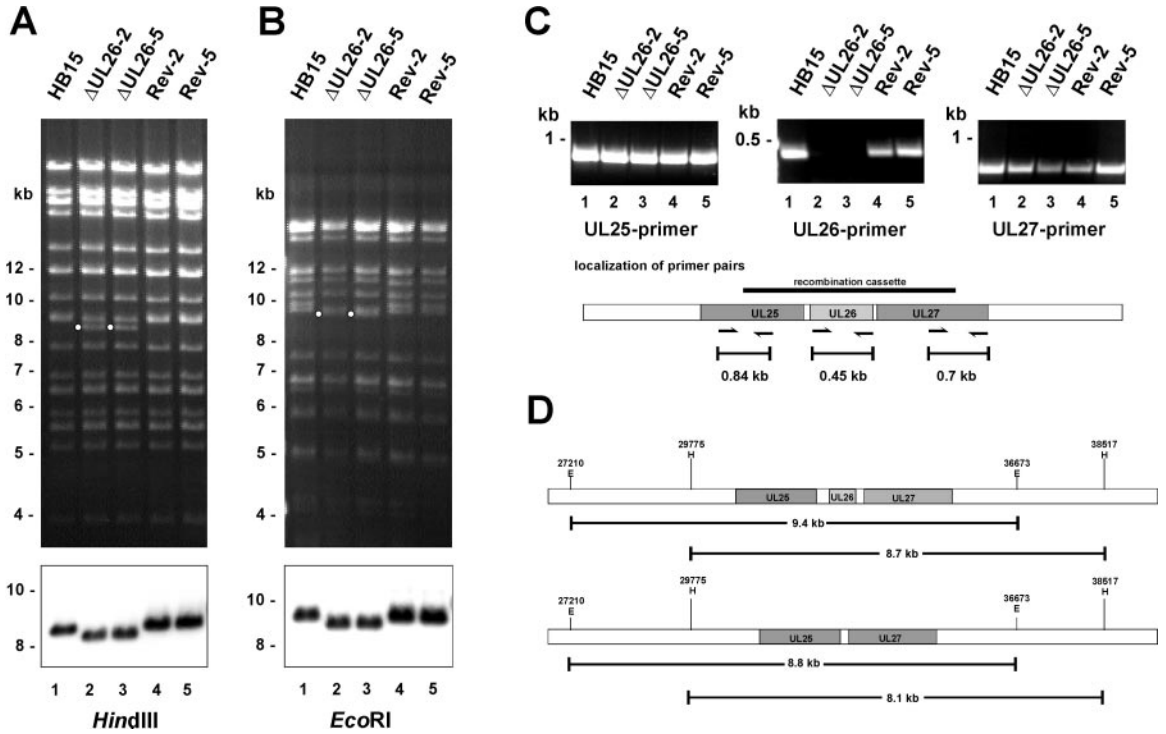

FIG. 1. Structural analysis of HCMV BAC plasmids. (A and B) HindIII (A) and EcoRI (B) cleavage of wild-type (pHB15, lane 1), ΔUL26 (ΔUL26-2 and ΔUL26-5, lanes 2 and 3, respectively), and UL26 revertant (Rev-2 and Rev-5, lanes 4 and 5, respectively) BACs. The fragments unique to ΔUL26 are marked with dots. Southern blot analyses from BAC DNAs treated with HindIII and EcoRI using a biotinylated probe comprising the UL25-UL27 genomic region are shown in the bottom panels. Molecular size markers are indicated. (C) For verification of the correct recombination sites within the HCMV genome, PCR analyses of bacterial clones harboring the indicated BACs were performed using oligonucleotides specific for UL25 (left panel), UL26 (middle panel), and UL27 (right panel), respectively. The location of the primers in relation to the recombination cassette is shown in the scheme below. Lanes: 1, PCR with wild-type BAC pHB15; 2 and 3, PCRs with UL26 deletion BACs ΔUL26-2 and ΔUL26-5, respectively; 4 and 5, PCRs with revertant BACs Rev-2 and Rev-5, respectively. The scheme in D shows the HindIII and EcoRI restriction sites in relation to the relevant genomic segments of HCMV.

successfully deleted UL26 and generated a revertant virus with a reinsertion of the UL26 ORF.

Reconstitution and protein expression of recombinant viruses. To test whether the recombinant BACs could be reconstituted to infectious viruses, primary HFF cells were transfected with purified DNA of the ΔUL26 BAC, the revertant BAC, or pHB15 as a control. One week after transfection, the cells were transferred to 25-cm^2 flasks and cultured for about 2 weeks until plaques appeared. Subsequently, the viral supernatants were used to infect fresh HFF cultures for the preparation and titration of virus stocks. Infectious particles could be reconstituted from all recombinant BACs, including the ΔUL26 BAC, indicating that the UL26 ORF is not absolutely necessary for viral growth. It was conspicuous, however, that plaque appearance and CPE development were repeatedly delayed in cells transfected with ΔUL26 BACs compared to wild-type pHB15 and the UL26 revertant BACs.

To show that the UL26 deletion mutant was no longer able to express the UL26 protein and that the regions adjacent to UL26 were not affected, infected cells were harvested and lysed after the cultures displayed a distinct CPE. Lysates from mock-infected cells or HFF cells infected with HB15, Rev (UL26 revertant), and ΔUL26 were then subjected to Western blot analyses. The membranes were probed with either anti-UL26 serum (Fig. 2A), anti-UL25 MAb (Fig. 2B), or anti-UL69 serum (Fig. 2C). Neither the 21- nor the 27-kDa isoform of pUL26 could be detected with the ΔUL26 virus (Fig. 2A, lane 4), whereas both isoforms were expressed in cells infected with HB15 wild-type and the UL26 revertant viruses (lanes 2 and 3, respectively). Expression of pUL25 by ΔUL26, Rev, and wild-type HB15 showed that the disruption of the UL26 ORF did not affect the adjoining UL25 gene region (Fig. 2B, lanes 2 to 4). Confirmation of pUL27 protein expression was not possible, as no antiserum against this protein has been described in the literature so far. However, we were able to detect RNA expression from the UL27 gene region by reverse transcription-PCR, indicating that gene expression from this region is not impaired by the deletion of UL26 (Fig. 2D). Aside from pUL26 and pUL25, we examined the expression of an additional tegument protein, ppUL69, which was present in all viral lysates (Fig. 2C, lanes 2 to 4). In summary, these experiments confirm the absence of pUL26 expression after infection with the ΔUL26 virus as well as the successful reinsertion of the UL26 ORF in the revertant virus.

DNA and protein accumulation after infection with ΔUL26. Since our previous results suggested that pUL26 could affect the initiation of immediate-early gene expression, we wanted to investigate the accumulation of viral proteins and DNA during the replication cycle of ΔUL26. Due to the potential defect of ΔUL26 in IE gene expression, we decided to perform

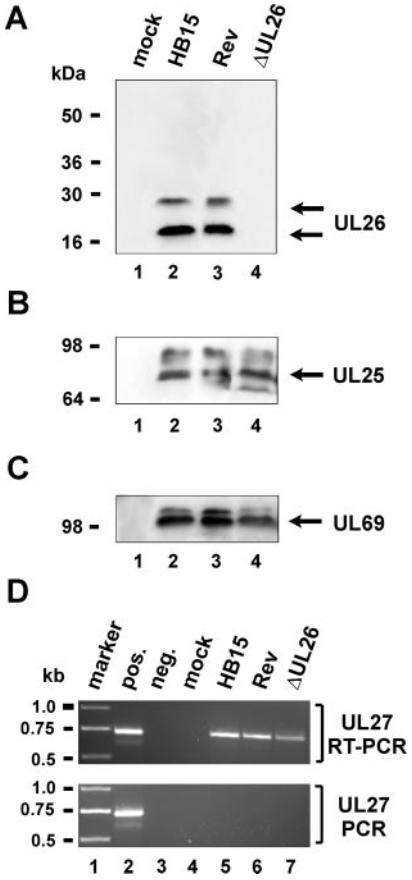

FIG. 2. Analysis of protein and RNA expression of recombinant viruses. (A to C) HFF cells were mock infected (lane 1) or infected with HB15 (lane 2), Rev (lane 3), or ΔUL26 (lane 4) and harvested after confluent spreading of the CPE. Afterwards, the expression of pUL26 (A), pUL25 (B), and pUL69 (C) was examined by Western blot analyses using specific antibodies against the respective proteins. Molecular size markers are given at the left of each panel. (D) Reverse transcription-PCR analysis of UL27 RNA expression. (Upper panel) RNA of infected cells was reverse transcribed, followed by PCR amplification using UL27-specific primers. (Lower panel) PCR amplification was performed without prior reverse transcription of RNA. marker, molecular size marker; pos., HCMV DNA, used as a positive control for the PCR; neg., no DNA was added; mock, RNA from mock-infected cells; HB15, RNA from HB15-infected cells; Rev, RNA from Rev-infected cells; ΔUL26, RNA from ΔUL26-infected cells.

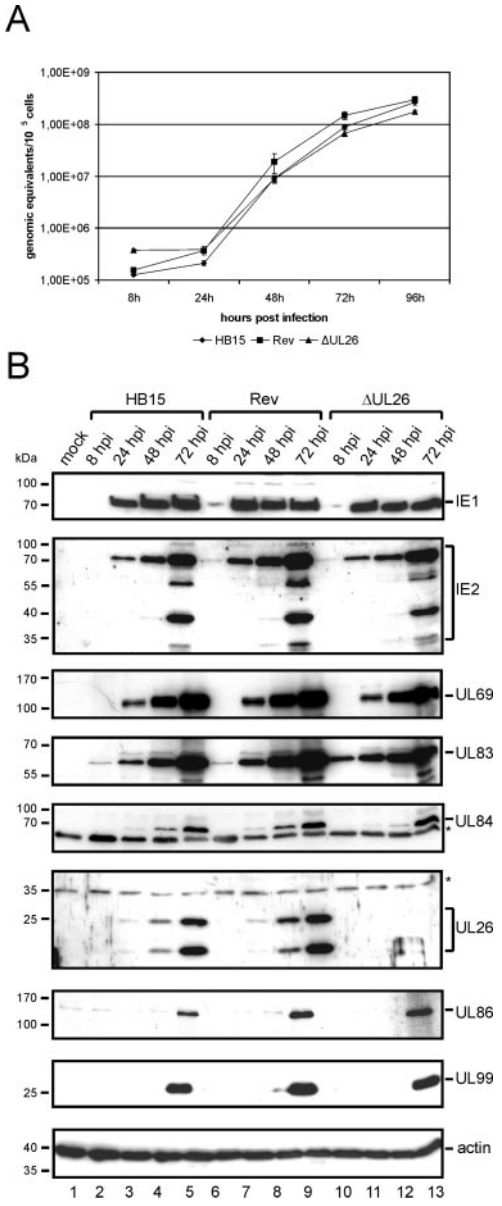

FIG. 3. Accumulation of viral DNA and protein after infection with recombinant viruses. Infection was performed with viral inocula that were normalized for an equivalent uptake of viral DNA into cells. DNA and protein were harvested at 8, 24, 48, 72, and 96 h after infection. (A) HCMV-specific real-time PCR was performed to quantify viral genomes during the replicative cycle of HB15, Rev, or ΔUL26. Experiments were performed in triplicate; standard deviations are indicated. (B) Western blot analyses were performed to monitor the accumulation of viral proteins during the replicative cycle of HB15 (lanes 2 to 5), Rev (lanes 6 to 9), or ΔUL26 (lanes 10 to 13). The detected proteins are indicated at the right of each panel, nonspecific bands are indicated by asterisks, the sizes of molecular mass markers are given on the left. hpi, hours postinfection.

infection experiments with viral inocula that were normalized for equivalent uptake of viral DNA by infection. For this, HFFs were infected at an MOI of 0.1 with wild-type virus HB15 and various dilutions of ΔUL26 and the revertant virus. TaqMan PCR was then performed to quantify viral genomes within cellular DNA that was extracted 12 h after infection. In subsequent experiments, infections were performed with viral inocula that were normalized to result in an equivalent uptake of viral genomes. In a first series of experiments, we investigated whether the accumulation of viral progeny DNA is impaired after infection with ΔUL26. As shown in Fig. 3A, we observed no significant difference in the kinetics of viral DNA accumulation between wild-type, mutant, and revertant viruses. This excludes a major effect of pUL26 on viral DNA replication. Protein accumulation was then monitored by Western blotting, again using infection conditions that were normalized for the uptake of viral DNA. As expected, no UL26 protein was detected after infection with ΔUL26 (Fig. 3B, lanes 10 to 13). Surprisingly, however, immediate-early (IE1 and IE2), early (UL69, UL83, and UL84), and late (UL86 and UL99) proteins accumulated to approximately wild-type levels

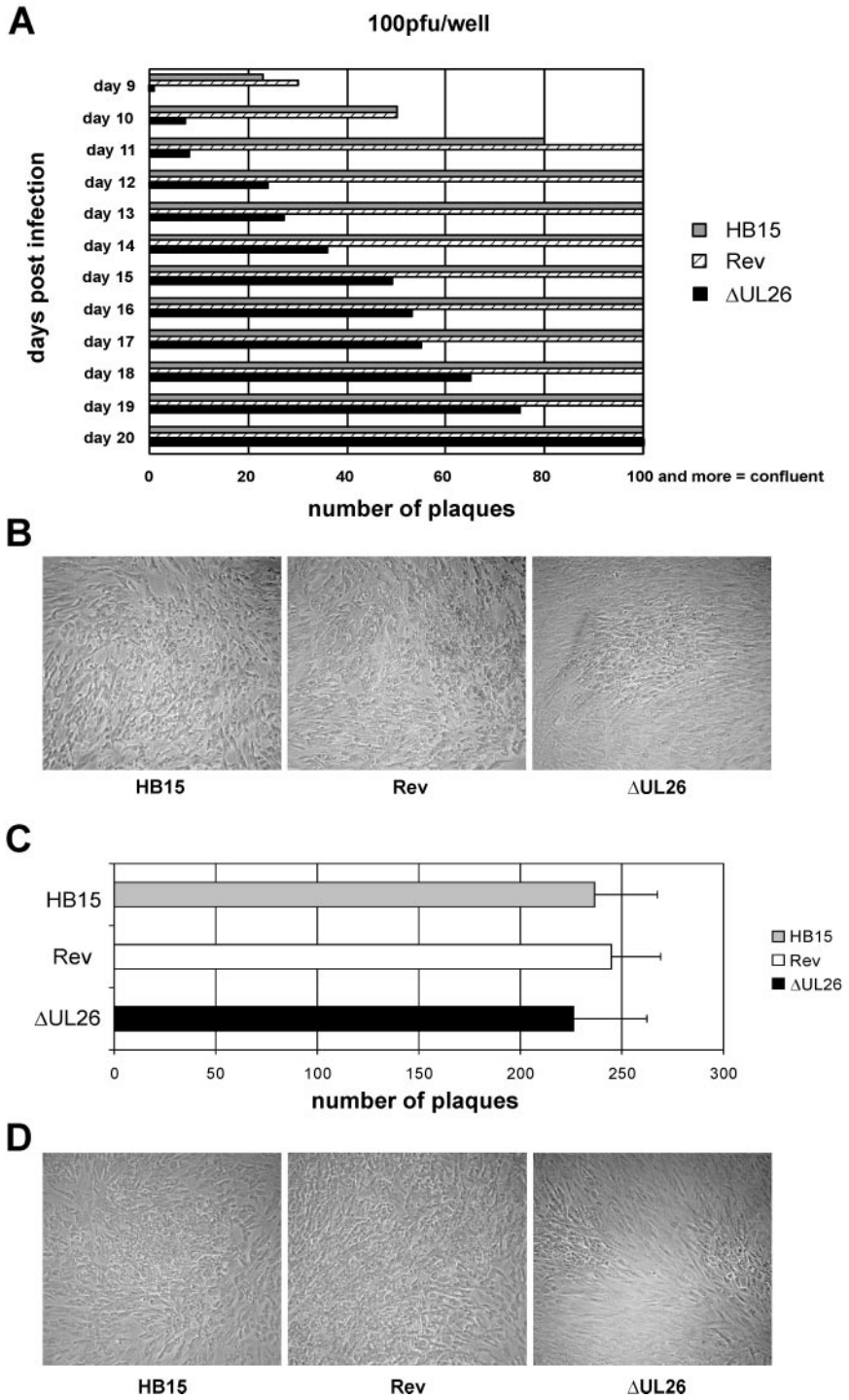

FIG. 4. Analysis of plaque formation of recombinant viruses. (A) HFF cells were infected in duplicate with the recombinant viruses HB15 (gray bars), Rev (striped bars), and ΔUL26 (black bars) at 0.0005 infectious units/cell. The infection was followed by a conventional plaque overlay assay. After the appearance of plaques, the plaques for each virus were counted every day until confluence. Given are the mean plaque numbers for each duplicate infection. (B) Shown is a comparison of representative plaques in cultures infected with HB15, Rev, and ΔUL26 at day 15 postinfection. (C) IE1p72-expressing cells were infected in triplicate with HB15 (gray bar), Rev (white bar), or ΔUL26 (black bar) at 0.0005 infectious units/cell followed by a plaque overlay assay. The graph represents the number of plaques determined at day 12 after infection; standard deviations are indicated. (E) Shown is a comparison of representative plaques after infection of IE1p72-expressing cells with HB15, Rev, and ΔUL26 at day 12 postinfection.

in the absence of UL26 (Fig. 3B). Thus, the results observed during one round of viral replication at an MOI of 0.1 did not support the notion that pUL26 is involved in the regulation of HCMV IE gene expression.

Analysis of plaque formation. During reconstitution of infectious viruses, we repeatedly noticed a clearly slower plaque formation in cultures containing the ΔUL26 virus. In order to study the kinetics of plaque formation in more detail, HFF cells were infected with 0.0005 infectious units/cell of HB15, Rev, and ΔUL26 viruses. The viral inoculum was removed after 1.5 h, and the cells were covered with agarose overlay medium and subsequently incubated at 37°C until the first plaques were visible for all viruses (Fig. 3A, day 9 postinfection). Afterwards, the plaque numbers for each virus were counted daily until the cultures showed a complete confluence of plaques. In Fig. 3A, mean plaque numbers from infections performed in duplicate are shown additively for each recombinant virus. Compared to HB15 and Rev, we detected a significantly lower number of plaques for ΔUL26 at each time point. Furthermore, cells infected with the revertant and wild-type viruses showed confluence of plaques at day 12, whereas for ΔUL26, this was not observed before day 20. In addition, the sizes of plaques induced by the ΔUL26 mutant were on average significantly smaller than those of the wild-type and revertant viruses (Fig. 3B). Comparable results were obtained in experiments using 0.00025 or 0.001 infectious units/cell as an inoculum (data not shown). Thus, the UL26 deletion mutant displayed a significant delay in plaque formation, indicating that pUL26 plays an important role during viral replication, at least under conditions of a low MOI.

Although we were not able to observe a delay in IE gene expression after infection with ΔUL26 at an MOI of 0.1, it could still be possible that pUL26 plays a role in the initiation of viral gene expression at a lower MOI. In order to investigate whether the observed plaque phenotype of ΔUL26 could be rescued by the expression of IE1p72, a pool of primary human fibroblasts expressing IE1p72 was generated via retroviral transduction. These cells efficiently complemented the growth defect of IE1 deletion mutant CR208 (data not shown). Plaque assays were then performed by infection with 0.0005 infectious units/cell as described above. At day 12 after infection, the number of plaques was determined for HB15, Rev, and ΔUL26. Interestingly, while we observed a generally increased number of plaques for both wild-type and mutant viruses on IE1p72-expressing cells, the number of plaques determined for ΔUL26 was equivalent to the number of plaques determined for HB15 and Rev, indicating that the coexpression of IE1p72 could augment the growth of ΔUL26 (Fig. 4C). In contrast, however, the small-plaque phenotype was not rescued by IE1p72 (Fig. 4D), suggesting that ΔUL26 may have an additional defect during later stages of the replicative cycle that affects the spread of infection in cell culture.

Growth kinetics of mutant and revertant viruses. In order to investigate the observed delay in CPE development of the ΔUL26 virus more precisely, multistep growth curves were generated. Due to the results obtained in plaque assays with IE1p72-expressing cells, we were particularly interested to investigate whether the loss of pUL26 also affects stages of viral replication after the onset of IE transcription. Therefore, viral inocula used in these experiments were standardized for comparable IE1p72 expression (4). First, we performed an experiment to compare the yields of wild-type, revertant, and ΔUL26 viruses at 9 days after infection using two different MOIs; this was done in order to investigate whether the growth of ΔUL26 is MOI dependent. For this, infections were performed at MOIs of 0.1 or 0.01 infectious units/cell. Infection at a higher multiplicity was not possible due to the low viral titers produced by ΔUL26; even for infection at an MOI of 0.1, viral supernatants of ΔUL26 had to be concentrated via ultrafiltration. As shown in Fig. 5A, infection with ΔUL26 at an MOI of either 0.1 or 0.01 resulted in reduced viral yields compared to those of wild-type and revertant viruses, but the drop at an MOI of 0.01 was clearly more pronounced, indicating that ΔUL26 shows MOI-dependent growth.

Detailed growth kinetics of all viruses were then compared at an MOI of 0.01. Aliquots from the supernatant of the infected cells were taken at 1, 3, 5, 7, 9, and 12 days after inoculation for determination of viral titers via IE1p72 staining. Figure 5B shows that ΔUL26 replicated to titers about 1 log lower than wild-type and revertant viruses until day 7 postinfection. Strikingly, we observed a strong decline of ΔUL26 titers after day 7 postinfection, whereas titers of the other viruses still slightly increased. As the revertant virus Rev exhibited nearly identical growth kinetics compared to HB15, we concluded that the phenotype of ΔUL26 was indeed due to the deletion of the UL26 ORF and not to an unintentional mutation within the HCMV genome.

The striking decline of the growth of the ΔUL26 virus after day 7 could be caused by reduced infectivity due to an instability of the virus particles. For a further investigation of infectivity in the culture supernatants, a physical parameter for measurement was necessary, and we therefore decided to quantify virus particles by viral genomic equivalents as determined by real-time PCR. For this, DNA was extracted from aliquots of each viral supernatant obtained from the growth curve experiment shown in Fig. 5B, followed by quantification of viral DNA by real-time PCR (Fig. 5C). Both HB15 and Rev showed a nearly identical release of genomes until day 12. However, a higher amount of viral DNA for ΔUL26 was detected at day 1 postinfection compared to the other viruses, although equivalent infectious doses had been used for the inoculation, suggesting that the viral inoculum of ΔUL26 contained a high number of noninfectious particles. Surprisingly, however, the reduction of ΔUL26 infectious titers as observed in Fig. 5B after day 7 was not reflected by a diminished release of viral genomes. In contrast, the genomic equivalents of ΔUL26 also increased until day 12 postinfection (compare Fig. 5B and C). One possible explanation for this discrepancy could be a reduced stability of viral particles due to the lack of incorporation of pUL26 into the tegument. In the case of a virus with reduced stability, more particles would be required to gain the same infectious dose, thus resulting in a higher amount of genomic equivalents present in the inoculum.

Analysis of ΔUL26 virion stability. In order to address the question of reduced viral particle stability, we infected HFF cells at 0.001 infectious units/cell with freshly thawed viral supernatants containing either HB15, Rev, or ΔUL26 in duplicate (day 0). For the following 5 days, cells were infected in duplicate with the same virus stocks, which had meanwhile been incubated at 20°C. At 48 h postinfection, IE1p72 quan-

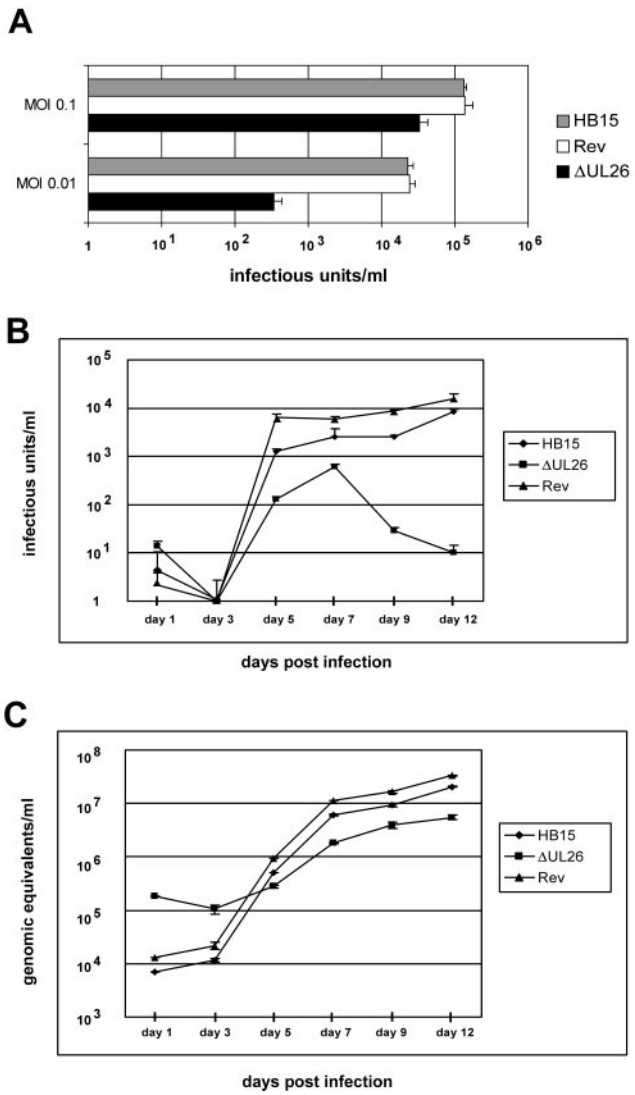

FIG. 5. Growth kinetics of the recombinant viruses. For infection of HFF cells, the viral inoculum was standardized for equal IE1p72 expression 24 h postinfection. (A) HFFs were infected in parallel with HB15, Rev, or ΔUL26 at an MOI of either 0.1 or 0.01. Cell culture supernatants were harvested at 9 days postinfection, followed by quantification of infectious virus via IE1p72 fluorescence (see Materials and Methods). Error bars indicate standard deviations. (B) Multistep growth curves were performed using 0.01 infectious units/cell of the indicated recombinant viruses in triplicate. The supernatants were harvested at days 1, 3, 5, 7, 9, and 12 postinfection and frozen at −80°C. After thawing, the probes were again titrated via IE1p72 expression in triplicate. Standard deviations are indicated on the graph. (C) Quantification of viral genomes in the supernatant of infected HFF cells by real-time PCR. Aliquots of the supernatants obtained for the multistep growth curve shown in B were treated with proteinase K, incubated at 56°C for 1 h, and subsequently denatured at 95°C. Five microliters of each lysate was subjected to real-time PCR to quantify the genomic equivalents in the supernatants of the recombinant viruses. Evaluation was performed in triplicate from each of the three infections per virus at each time point. Standard deviations are indicated.

tification was performed for each infection (4). Both values per virus are shown as distinct bars in Fig. 6. The percentage of remaining infectivity of viral supernatants at days 1 to 5 in relation to the infectivity at day 0, which was set as 100%, is

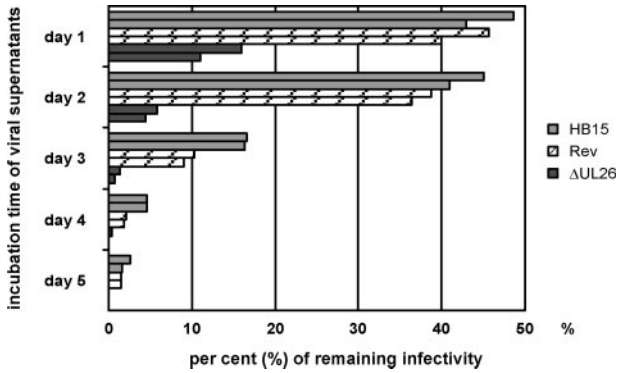

FIG. 6. Reduced stability of the ΔUL26 virus. HFF cells were infected with 0.001 infectious units/cell of freshly thawed supernatant of the recombinant viruses HB15 (gray bars), Rev (striped bars), and ΔUL26 (black bars). After 1 h of incubation, the viral supernatants were removed, and fresh medium was added. The remaining virus stocks were stored at 20°C and used for infection of HFF cells for the following 5 days. Subsequently, the number of IE1p72-positive cells was determined for each virus at each time point 48 h after the infection was started. The remaining infectivity shown on the *x* axis was related to the infectivity of the supernatants at day 0, which was set as 100%. Determination of cell numbers was carried out in duplicate (both values for each virus are depicted as bars).

given. Twenty-four hours and 48 h after virus stocks were thawed, HB15 and Rev still exhibited 40 to 50% infectivity, whereas the remaining infectivity for ΔUL26 was only approximately 15% (24 h) and 7% (48 h), respectively. Thus, the infectivity of the ΔUL26 virus declined significantly faster than HB15 wild-type or revertant viruses. Comparable results were obtained when the same experiment was repeated with virus stocks stored at 37°C (data not shown). These data strongly suggest a diminished stability of ΔUL26 virions in comparison to wild-type and revertant virus particles.

Analysis of the tegument composition and ultrastructure of ΔUL26 virions. Next, we wanted to investigate whether the tegument composition of ΔUL26 virions was altered in comparison to wild-type virus. Therefore, virions were purified from the supernatant of infected cell cultures by glycerol-tartrate gradient centrifugation (3) and subjected to Western blot experiments. In order to analyze an equal number of viral particles for wild-type and mutant viruses, we first adjusted the protein amount of the virion preparations to comparable MCP content (Fig. 7A, lanes 2 and 3). As confirmed previously, both isoforms of pUL26 were lacking from the deletion virus (Fig. 7B, lane 3). When antibodies against the tegument proteins pUL24, pUL25, ppUL69, pp65(UL83), and pp28(UL99) were used, no significant difference in the amount of these proteins was detected between ΔUL26 and wild-type virions (Fig. 7C to G). Surprisingly, however, we observed a markedly increased amount of the regulatory tegument protein pp71(UL82) in ΔUL26 virions (Fig. 7H, lane 3). Since this result was obtained from several independent experiments (data not shown), it is conceivable that a higher concentration of pp71(UL82) in the tegument of virus particles might compensate for the lack of pUL26.

Since this result suggested that virus assembly of ΔUL26 may be impaired, we decided to investigate the ultrastructure of particle maturation by electron microscopy using HFFs in-

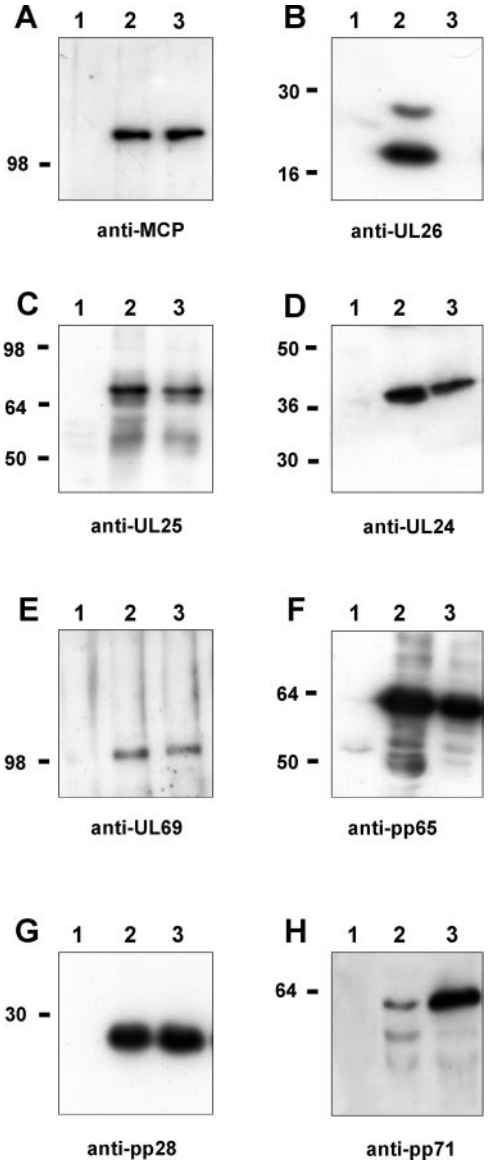

FIG. 7. Tegument protein composition of wild-type (HB15) and mutant (ΔUL26) virions. Virus particles from the supernatant of HFF cells infected with HB15 or ΔUL26 were separated from cell fragments via low-speed centrifugation. Thereafter, the particles were purified by sedimentation in a glycerol-tartrate gradient, thus resulting in virion fractions, which were used for immunoblot analyses. Virion proteins were detected using monoclonal antibodies against MCP(UL86) (A), pUL25 (C), pUL24 (D), pp65(UL83) (F), and pp28(UL99) (G) or polyclonal antisera against pUL26 (B), ppUL69 (E), and pp71(UL82) (H). Lane 1 contains lysates of mock-infected cells, lane 2 contains lysates of HB15-infected cells, and lane 3 contains lysates of ΔUL26-infected cells (A to H).

fected with wild-type HB15 or mutant ΔUL26 virus. Infection was stopped at 72 h postinfection, and cells were prepared for electron microscopy. Analysis of the nuclei of infected cells showed that all three types of capsids (A-, B-, and C-type capsids) were present (Fig. 8a and b). In addition, no significant difference in the number of capsids was observed within the nuclei. However, while we could easily detect mature enveloped viral particles within the cytoplasm of HB15-infected cells (Fig. 8c), only very few enveloped particles were found in the cytoplasm of cells infected with ΔUL26. In contrast, many immature viral particles could be observed in the cytoplasm of ΔUL26-infected cells that were in part associated with electron-dense structures (Fig. 8d). In extracellular virion preparations, it was striking that most ΔUL26 virions appeared to be nonenveloped and defective (Fig. 8f), whereas with HB15, fully enveloped particles were easily detectable (Fig. 8e). These observations are consistent with our biochemical characterization of ΔUL26 virion instability and suggest an important role for pUL26 in the correct tegumentation of virus particles.

DISCUSSION

We have previously shown that the protein encoded by ORF UL26 of human cytomegalovirus contains a strong transcriptional activation domain and is incorporated into the tegument of infectious viral particles (44). Since this suggested an important function of pUL26 in replication, we decided to construct a mutant virus with a deletion of the entire UL26 ORF. Characterization of this mutant virus, termed ΔUL26, revealed a small-plaque phenotype together with a significant retardation of plaque formation. This defect in viral replication could be reversed by the reinsertion of UL26 into the mutant genome; furthermore, it was confirmed that expression of the adjoining open reading frames, UL25 and UL27, was not affected by the deletion. This indicates that the deletion of UL26 is the sole reason for the observed phenotype, which is consistent with the results of two large-scale studies that also described a severe growth defect after either insertion or deletion mutagenesis of this ORF (19, 52).

Due to the retarded plaque formation, it was not possible to reliably quantify viral titers via classical plaque assays. Therefore, we employed two different strategies for the quantification of the viral inoculum, namely, real-time PCR for determination of viral genome equivalents either in the supernatant of infected cells or within infected cells and the determination of IE1p72 expression (4). Both techniques have been used previously to detect defects in both IE gene expression and late processes in a recombinant virus lacking the UL35 tegument protein (38). Concerning the transactivating function of pUL26 on the HCMV MIEP (44), our experiments with ΔUL26 do not unequivocally demonstrate a contribution of pUL26 to the initiation of IE gene expression. After infection at an MOI of 0.1, no delay in IE gene expression could be detected, which would argue against a role for pUL26 in the initiation of viral IE gene expression; however, since we observed that ΔUL26 virions contain a significantly higher amount of pp71, which also functions as an activator of IE gene expression (12), the lack of pUL26 could be compensated for by pp71, particularly under conditions of a high MOI. In contrast, under conditions of a low MOI, we found that coexpression of IE1p72 was able to partially rescue the plaque phenotype of ΔUL26, since the number of plaques was considerably increased by coexpression of IE1p72. This suggests that pUL26 may indeed play a role in the initiation of viral IE gene expression, which is also supported by our previous observation that pUL26 acts as a transactivator of the major immediate-early enhancer-promoter (44). Interestingly, however, the small-plaque phenotype of ΔUL26 was not rescued by coexpression of IE1p72, suggesting

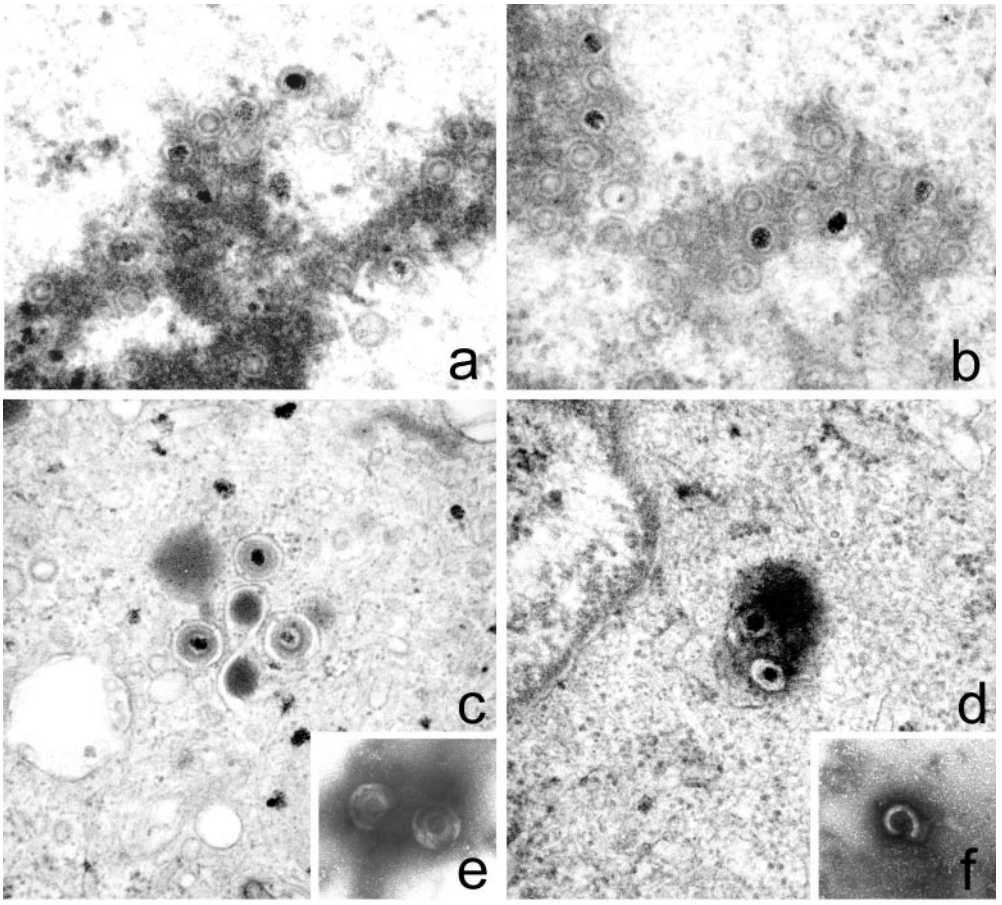

FIG. 8. Ultrastructural analysis of virus maturation and morphology. (a to d) HFF cells were infected with HB15 or ΔUL26 at an MOI of 0.5. Cells were fixed at 72 h postinfection and processed for electron microscopy. (a and b) Nuclei of HB15- and ΔUL26-infected cells, respectively. (c and d) Cytoplasm of HB15-and ΔUL26-infected cells. (e and f) Purified extracellular viral particles were visualized by negative staining with uranyl acetate. (e) HB15 virions. (f) ΔUL26 virion. All images were taken at ×46,460 magnification.

an additional defect that affects the spread of infection in cell culture. In order to detect a possible second defect of the ΔUL26 virus, we standardized the viral inocula for comparable IE1p72 expression (4), followed by determination of viral growth kinetics. This revealed only a moderately reduced release of infectious viral particles during the first 7 days after infection with ΔUL26. However, we detected a strong decrease of viral titers during further progression of infection. Surprisingly, when the release of viral DNA was quantified in parallel, we were not able to detect a decrease in viral genomes in the supernatant, which would explain the drop in infectious ΔUL26 virus titers (Fig. 5B and C). In contrast, viral DNA continued to accumulate in the supernatant after day 7 of infection in a way similar to that observed for wild-type and revertant viruses. This indicated that the release of physical viral particles was not diminished after infection with ΔUL26. We therefore concluded that the viral particles might be less infectious with prolonged incubation of viral supernatants, thus pointing towards a decreased stability of ΔUL26 virions. The incubation of viral supernatants at 20°C or 37°C for increasing time periods followed by determination of the residual infectivity indeed revealed a severely decreased half-life of the infectivity of extracellular ΔUL26 virions compared to those of wild-type and revertant viruses (Fig. 6 and data not shown). This is also supported by our ultrastructural analyses of virion morphology that detected a high number of defective viral particles in purified virion preparations.

Thus, our results suggest that the lack of pUL26 leads to a drastically impaired stability of extracellular viral particles. In this respect, ΔUL26 differs from previously described mutant cytomegaloviruses with the deletion of genes encoding tegument proteins. For instance, the deletion of UL35 from the HCMV genome also resulted in a severe growth defect, which was, however, due to a reduced release of infectious particles from cells (38). The growth defect after the deletion of UL35 was shown to be MOI dependent (38). Due to the impaired stability of ΔUL26 particles, it was difficult to obtain high-titered viral stocks. We were able to generate viral stocks that allowed us to perform infections at an MOI of 0.1 only via the concentration of cell culture supernatants by ultrafiltration. Although mutant ΔUL26 virus did not reach yields equivalent to those of wild-type and revertant viruses under infection conditions at an MOI of 0.1, we could clearly observe a stronger decrease of viral yields at a lower MOI, indicating MOI-dependent growth of ΔUL26.

Another tegument protein with recently proven importance

for the efficient assembly of viral particles is pTRS1 (1, 11). Although pTRS1 was initially described as a transcriptional activator that stimulates gene expression in conjunction with the immediate-early proteins IE1p72 and IE2p86 (45), analysis of a TRS1-deleted virus revealed no delay in the accumulation of viral RNAs and proteins but did reveal a major defect at late times of the replicative cycle, which was further narrowed down to a role for pTRS1 in the assembly of DNA-containing capsids (1). However, the kinetics of viral DNA release in the supernatant of ΔUL26-infected cells argue against an involvement of pUL26 in either capsid assembly or the loading of DNA into capsids.

Rather, since the major defect observed with ΔUL26 was impaired viral particle stability, we hypothesize that the lack of pUL26 compromises the correct tegumentation of HCMV. While the herpesviral tegument has long been considered an unstructured protein accumulation, there is increasing evidence that an intricate network of protein-protein interactions is important for proper assembly of this structure (reviewed in reference 28). Although a built-in redundancy may be responsible for tolerating the lack of some tegument proteins, like the abundant phosphoprotein pp65(UL83) (40), there are now several reports of polypeptides with an essential function in the tegumentation of HCMV (13, 29, 41). Moreover, several protein-protein interactions between tegument proteins and between tegument and capsid proteins have recently been described (9, 10, 39). For instance, it was shown that the HCMV UL47 tegument protein coimmunoprecipitates with the tegument proteins pUL48 and pUL69 as well as MCP(UL86), thus suggesting the existence of a protein complex (10). Interestingly, viral particles of a UL47-deleted virus contained significantly lower amounts of pUL48, indicating that protein interactions are responsible for the correct incorporation of tegument proteins into viral particles. In this respect, analysis of the protein composition of ΔUL26 virions revealed a markedly increased amount of pp71(UL82) protein, while several other tegument polypeptides, like pUL24, pUL25, pUL69, pp65(UL83), and pp28(UL99), were not altered in abundance. One may hypothesize that pUL26 acts to downregulate the incorporation of pp71(UL82) into the tegument of virus particles, possibly by competing with pp71(UL82) for binding to another structural virion component. A further detailed analysis of protein interactions between pUL26 and other viral structural and nonstructural proteins will be necessary to clarify which step is affected by pUL26 during tegumentation.

In summary, we describe that the deletion of UL26 from the HCMV genome results in viral particles with an altered tegument composition and severely reduced stability, which is a novel way to explain how the lack of a tegument protein impairs viral growth. Our results add further evidence to the concept that individual tegument proteins play an important role in the correct assembly of viral particles and the stability of extracellular virions.

ACKNOWLEDGMENTS

We thank Michael Winkler for critical reading of the manuscript and K. Metzner and H. Reil for help with the TaqMan PCR. We also thank B. Britt, D. J. Dargan, G. Hahn, M. P. Landini, and A. F. Stewart for providing plasmids and antibodies.

This work was supported by the Deutsche Forschungsgemeinschaft (SFB473), the IZKF Erlangen, and the Wilhelm Sander Stiftung.

REFERENCES

1. **Adamo, J. E., J. Schroer, and T. Shenk.** 2004. Human cytomegalovirus TRS1 protein is required for efficient assembly of DNA-containing capsids. J. Virol. **78:**10221–10229.
2. **Adler, H., M. Messerle, and U. H. Koszinowski.** 2003. Cloning of herpesviral genomes as bacterial artificial chromosomes. Rev. Med. Virol. **13:**111–121.
3. **Almeida, J., D. Lang, and P. Talbot.** 1978. Herpesvirus morphology: visualization of a structural subunit. Intervirology **10:**318–320.
4. **Andreoni, M., M. Faircloth, L. Vugler, and W. J. Britt.** 1989. A rapid microneutralization assay for the measurement of neutralizing antibody reactive with human cytomegalovirus. J. Virol. Methods **23:**157–167.
5. **Arlt, H., D. Lang, S. Gebert, and T. Stamminger.** 1994. Identification of binding sites for the 86-kilodalton IE2 protein of human cytomegalovirus within an IE2-responsive viral early promoter. J. Virol. **68:**4117–4125.
6. **Baldick, C. J., Jr., A. Marchini, C. E. Patterson, and T. Shenk.** 1997. Human cytomegalovirus tegument protein pp71 (ppUL82) enhances the infectivity of viral DNA and accelerates the infectious cycle. J. Virol. **71:**4400–4408.
7. **Baldick, C. J., Jr., and T. Shenk.** 1996. Proteins associated with purified human cytomegalovirus particles. J. Virol. **70:**6097–6105.
8. **Battista, M. C., G. Bergamini, M. C. Boccuni, F. Campanini, A. Ripalti, and M. P. Landini.** 1999. Expression and characterization of a novel structural protein of human cytomegalovirus, pUL25. J. Virol. **73:**3800–3809.
9. **Baxter, M. K., and W. Gibson.** 2001. Cytomegalovirus basic phosphoprotein (pUL32) binds to capsids in vitro through its amino one-third. J. Virol. **75:**6865–6873.
10. **Bechtel, J. T., and T. Shenk.** 2002. Human cytomegalovirus UL47 tegument protein functions after entry and before immediate-early gene expression. J. Virol. **76:**1043–1050.
11. **Blankenship, C. A., and T. Shenk.** 2002. Mutant human cytomegalovirus lacking the immediate-early TRS1 coding region exhibits a late defect. J. Virol. **76:**12290–12299.
12. **Bresnahan, W. A., and T. E. Shenk.** 2000. UL82 virion protein activates expression of immediate early viral genes in human cytomegalovirus-infected cells. Proc. Natl. Acad. Sci. USA **97:**14506–14511.
13. **Britt, W. J., M. Jarvis, J. Y. Seo, D. Drummond, and J. Nelson.** 2004. Rapid genetic engineering of human cytomegalovirus by using a lambda phage linear recombination system: demonstration that pp28 (UL99) is essential for production of infectious virus. J. Virol. **78:**539–543.
14. **Chee, M. S., A. T. Bankier, S. Beck, R. Bohni, C. M. Brown, R. Cerny, T. Horsnell, C. A. Hutchison, T. Kouzarides, J. A. Martignetti, E. Preddie, S. C. Satchwell, P. Tomlinson, K. M. Weston, and B. G. Barell.** 1990. Analysis of the protein-coding content of the sequence of human cytomegalovirus strain AD169. Curr. Top. Microbiol. Immunol. **154:**125–169.
15. **Cherepanov, P. P., and W. Wackernagel.** 1995. Gene disruption in Escherichia coli: TcR and KmR cassettes with the option of Flp-catalyzed excision of the antibiotic-resistance determinant. Gene **158:**9–14.
16. **Colberg-Poley, A. M., L. D. Santomenna, P. P. Harlow, P. A. Benfield, and D. J. Tenney.** 1992. Human cytomegalovirus US3 and UL36-38 immediate-early proteins regulate gene expression. J. Virol. **66:**95–105.
17. **Davison, A. J., A. Dolan, P. Akter, C. Addison, D. J. Dargan, D. J. Alcendor, D. J. McGeoch, and G. S. Hayward.** 2003. The human cytomegalovirus genome revisited: comparison with the chimpanzee cytomegalovirus genome. J. Gen. Virol. **84:**17–28.
18. **DeMarchi, J. M.** 1981. Human cytomegalovirus DNA: restriction enzyme cleavage maps and map locations for immediate-early, early, and late RNAs. Virology **114:**23–38.
19. **Dunn, W., C. Chou, H. Li, R. Hai, D. Patterson, V. Stolc, H. Zhu, and F. Liu.** 2003. Functional profiling of a human cytomegalovirus genome. Proc. Natl. Acad. Sci. USA **100:**14223–14228.
20. **Griffiths, P. D.** 1996. Herpesviruses and AIDS. Scand. J. Infect. Dis. Suppl. **100:**3–7.
21. **Hermiston, T. W., C. L. Malone, P. R. Witte, and M. F. Stinski.** 1987. Identification and characterization of the human cytomegalovirus immediate-early region 2 gene that stimulates gene expression from an inducible promoter. J. Virol. **61:**3214–3221.
22. **Ho, M.** 1991. Cytomegalovirus biology and infection. Plenum Medical Book Co., New York, N.Y.
23. **Hobom, U., W. Brune, M. Messerle, G. Hahn, and U. H. Koszinowski.** 2000. Fast screening procedures for random transposon libraries of cloned herpesvirus genomes: mutational analysis of human cytomegalovirus envelope glycoprotein genes. J. Virol. **74:**7720–7729.
24. **Liu, B., and M. F. Stinski.** 1992. Human cytomegalovirus contains a tegument protein that enhances transcription from promoters with upstream ATF and AP-1 *cis*-acting elements. J. Virol. **66:**4434–4444.
25. **McDonough, S. H., and D. H. Spector.** 1983. Transcription in human fibroblasts permissively infected by human cytomegalovirus strain AD169. Virology **125:**31–46.
26. **Meier, J. L., and M. F. Stinski.** 1996. Regulation of human cytomegalovirus immediate-early gene expression. Intervirology **39:**331–342.
27. **Messerle, M., I. Crnkovic, W. Hammerschmidt, H. Ziegler, and U. H. Koszinowski.** 1997. Cloning and mutagenesis of a herpesvirus genome as an

infectious bacterial artificial chromosome. Proc. Natl. Acad. Sci. USA **94:** 14759–14763.
28. **Mettenleiter, T. C.** 2002. Herpesvirus assembly and egress. J. Virol. **76:**1537–1547.
29. **Meyer, H. H., A. Ripalti, M. P. Landini, K. Radsak, H. F. Kern, and G. M. Hensel.** 1997. Human cytomegalovirus late-phase maturation is blocked by stably expressed UL32 antisense mRNA in astrocytoma cells. J. Gen. Virol. **78:**2621–2631.
30. **Muyrers, J. P., Y. Zhang, V. Benes, G. Testa, W. Ansorge, and A. F. Stewart.** 2000. Point mutation of bacterial artificial chromosomes by ET recombination. EMBO Rep. **1:**239–243.
31. **Nicholas, J.** 1996. Determination and analysis of the complete nucleotide sequence of human herpesvirus. J. Virol. **70:**5975–5989.
32. **O'Connor, M., M. Peifer, and W. Bender.** 1989. Construction of large DNA segments in Escherichia coli. Science **244:**1307–1312.
33. **Pass, R. F.** 2001. Cytomegalovirus, p. 2675–2705. *In* D. M. Knipe, P. M. Howley, D. E. Griffin, R. A. Lamb, M. A. Martin, B. Roizman, and S. E. Straus (ed.), Fields virology, 4th ed. Lippincott Williams & Wilkins, Philadelphia, Pa.
34. **Pizzorno, M. C., M. A. Mullen, Y. N. Chang, and G. S. Hayward.** 1991. The functionally active IE2 immediate-early regulatory protein of human cytomegalovirus is an 80-kilodalton polypeptide that contains two distinct activator domains and a duplicated nuclear localization signal. J. Virol. **65:**3839–3852.
35. **Posfai, G., M. D. Koob, H. A. Kirkpatrick, and F. R. Blattner.** 1997. Versatile insertion plasmids for targeted genome manipulations in bacteria: isolation, deletion, and rescue of the pathogenicity island LEE of the *Escherichia coli* O157:H7 genome. J. Bacteriol. **179:**4426–4428.
36. **Sambrook, J., E. F. Fritsch, and T. Maniatis.** 1989. Molecular cloning: a laboratory manual, 2nd ed. Cold Spring Harbor Laboratory Press, Cold Spring Harbor, N.Y.
37. **Sanchez, V., E. Sztul, and W. J. Britt.** 2000. Human cytomegalovirus pp28 (UL99) localizes to a cytoplasmic compartment which overlaps the endoplasmic reticulum-Golgi-intermediate compartment. J. Virol. **74:**3842–3851.
38. **Schierling, K., C. Buser, T. Mertens, and M. Winkler.** 2005. Human cytomegalovirus tegument protein ppUL35 is important for viral replication and particle formation. J. Virol. **79:**3084–3096.
39. **Schierling, K., T. Stamminger, T. Mertens, and M. Winkler.** 2004. Human cytomegalovirus tegument proteins ppUL82 and ppUL35 interact and cooperatively activate the major immediate-early enhancer. J. Virol. **78:**9512–9523.
40. **Schmolke, S., H. F. Kern, P. Drescher, G. Jahn, and B. Plachter.** 1995. The dominant phosphoprotein pp65 (UL83) of human cytomegalovirus is dispensable for growth in cell culture. J. Virol. **69:**5959–5968.
41. **Silva, M. C., Q. C. Yu, L. Enquist, and T. Shenk.** 2003. Human cytomegalovirus UL99-encoded pp28 is required for the cytoplasmic envelopment of tegument-associated capsids. J. Virol. **77:**10594–10605.
42. **Skaletskaya, A., L. M. Bartle, T. Chittenden, A. L. McCormick, E. S. Mocarski, and V. S. Goldmacher.** 2001. A cytomegalovirus-encoded inhibitor of apoptosis that suppresses caspase-8 activation. Proc. Natl. Acad. Sci. USA **98:**7829–7834.
43. **Smith, S. R., D. W. Butterly, B. D. Alexander, and A. Greenberg.** 2001. Viral infections after renal transplantation. Am. J. Kidney Dis. **37:**659–676.
44. **Stamminger, T., M. Gstaiger, K. Weinzierl, K. Lorz, M. Winkler, and W. Schaffner.** 2002. Open reading frame UL26 of human cytomegalovirus encodes a novel tegument protein that contains a strong transcriptional activation domain. J. Virol. **76:**4836–4847.
45. **Stasiak, P. C., and E. S. Mocarski.** 1992. Transactivation of the cytomegalovirus ICP36 gene promoter requires the α gene product TRS1 in addition to IE1 and IE2. J. Virol. **66:**1050–1058.
46. **Stenberg, R. M., A. S. Depto, J. Fortney, and J. A. Nelson.** 1989. Regulated expression of early and late RNAs and proteins from the human cytomegalovirus immediate-early gene region. J. Virol. **63:**2699–2708.
47. **Varnum, S. M., D. N. Streblow, M. E. Monroe, P. Smith, K. J. Auberry, L. Pasa-Tolic, D. Wang, D. G. Camp, K. Rodland, S. Wiley, W. Britt, T. Shenk, R. D. Smith, and J. A. Nelson.** 2004. Identification of proteins in human cytomegalovirus (HCMV) particles: the HCMV proteome. J. Virol. **78:**10960–10966.
48. **Waldo, F. B., W. J. Britt, M. Tomana, B. A. Julian, and J. Mestecky.** 1989. Non-specific mesangial staining with antibodies against cytomegalovirus in immunoglobulin-A nephropathy. Lancet **i:**129–131.
49. **Wathen, M. W., D. R. Thomsen, and M. F. Stinski.** 1981. Temporal regulation of human cytomegalovirus transcription at immediate early and early times after infection. J. Virol. **38:**446–459.
50. **Winkler, M., S. Schmolke, B. Plachter, and T. Stamminger.** 1995. UL69 of HCMV, a homolog of the HSV ICP27, is contained within the tegument of virions and activates the major IE enhancer of HCMV in synergy with the tegument protein pp71(UL82). Scand. J. Infect. Dis. Suppl. **99:**8–9.
51. **Winkler, M., and T. Stamminger.** 1996. A specific subform of the human cytomegalovirus transactivator protein pUL69 is contained within the tegument of virus particles. J. Virol. **70:**8984–8987.
52. **Yu, D., M. C. Silva, and T. Shenk.** 2003. Functional map of human cytomegalovirus AD169 defined by global mutational analysis. Proc. Natl. Acad. Sci. USA **100:**12396–12401.